Article

X-ray Diffraction and DOSY NMR Characterization of Self-Assembled Supramolecular Metallocyclic Species in Solution

Tnde Megyes, Hershel Jude, Tams Grsz, Imre Bak, Tams Radnai, Gbor Trknyi, Gbor Plinks, and Peter J. Stang

J. Am. Chem. Soc., **2005**, 127 (30), 10731-10738• DOI: 10.1021/ja0523690 • Publication Date (Web): 06 July 2005

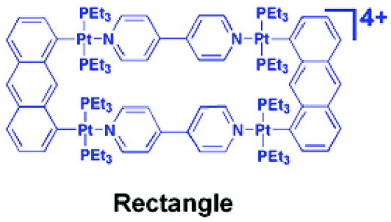

Rectangle

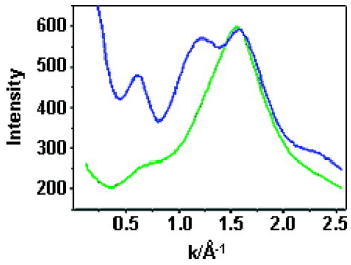

More About This Article

Additional resources and features associated with this article are available within the HTML version:

- Supporting Information
- Links to the 23 articles that cite this article, as of the time of this article download
- Access to high resolution figures
- Links to articles and content related to this article
- Copyright permission to reproduce figures and/or text from this article

View the Full Text HTML

Journal of the American Chemical Society is published by the American Chemical Society. 1155 Sixteenth Street N.W., Washington, DC 20036

J|A|C|S
ARTICLES
Published on Web 07/06/2005

X-ray Diffraction and DOSY NMR Characterization of Self-Assembled Supramolecular Metallocyclic Species in Solution

Tünde Megyes,[†] Hershel Jude,[‡] Tamás Grósz,[†] Imre Bakó,[†] Tamás Radnai,[†] Gábor Tárkányi,[†] Gábor Pálinkás,*[,†] and Peter J. Stang*[,‡]

Contribution from the Institute of Structural Chemistry, Chemical Research Center, Hungarian Academy of Sciences, P.O. Box 17, Budapest H-1525, Hungary, and Department of Chemistry, University of Utah, 315 South 1400 East, Room 2020, Salt Lake City, Utah 84112

Received April 12, 2005; E-mail: palg@chemres.hu; stang@chem.utah.edu

Abstract: Wide-angle X-ray scattering and diffusion NMR techniques have been used to obtain structural information on three self-assembled metallacyclic supramolecular complexes in solution: a rectangle, a triangle, and a three-diminsional cage. The low-angle region of the measured diffraction patterns and hydrodynamic radii calculations, determined from DOSY NMR experiments, suggest that the supramolecular assemblies retain their shape when dissolved in nitromethane. The experimental structure functions for the large-angle region have been analyzed, and the intramolecular contributions of the platinum−platinum interactions are discussed. These scattering measurements provide evidence that the supramolecular assemblies are not as rigid in solution as they are in the single crystal. Finally, by analysis of the radial distribution functions of the solutions, direct structural information (e.g., platinum−platinum intramolecular distances and coordination number) about the supramolecular assemblies has been obtained.

Introduction

Molecular self-assembly, the process whereby molecules spontaneously form ordered supramolecular ensembles via noncovalent interactions, is an area of considerable current interest and research activity due to its broad impact across a wide range of materials and biomimetic chemistry.[1−4] In this process the molecular structure, with its built-in recognition elements, determines the structure of the ordered supramolecular ensemble.

In the past dozen years, metal-driven and -directed self-assembly, taking advantage of the directionality of the metal−ligand dative interactions, has emerged as a major paradigm in abiological self-assembly.[5−17] This paradigm is well suited for the construction of both finite supramolecular species with well-defined structures and infinite networks such as grids, helicates, and the like.[5−17]

A major challenge in supramolecular chemistry and self-assembly, including the metal-directed approach, is proper structural characterization. This task is made all the more difficult by the complexity and nanoscale dimensions of supramolecular ensembles and architectures. Mass spectrometry and multinuclear NMR spectroscopy are most commonly employed to provide proof of composition and to deduce structural information, respectively. In cases where a suitable single crystal can be obtained, classical single-crystal X-ray diffraction provides the most reliable structural data, but only in the solid state.

An important question in the area of supramolecular chemistry and metal-directed self-assembly is the formation, shape, and structure of these species in solution. It is recognized that very weakly coordinated network solids form only in the solid state upon crystallization and do not exist as discrete species in solution.[18] However, with the development of modern electronics and high-speed computers, interest in liquid and solution structures of molecules has grown steadily.[19−31] Multinuclear NMR, by exploiting the nuclear Overhauser effect (NOE),

[†] Hungarian Academy of Sciences.
[‡] University of Utah.

(1) Whitesides, G. M.; Boncheva, M. *Proc. Natl. Acad. Sci. U.S.A.* **2002**, *99*, 4769−4774.
(2) Lehn, J.-M. *Proc. Natl. Acad. Sci. U.S.A.* **2002**, *99*, 4763−4768.
(3) Lehn, J. M. *Supramolecular Chemistry: Concepts and Perspectives*; VCH: New York, 1995.
(4) Lehn, J. M. In *The New Chemistry*; Hall, N., Ed.; Cambridge University Press: Cambridge, U.K., 2000; pp 200−251.
(5) Seidel, S. R.; Stang, P. J. *Acc. Chem. Res.* **2002**, *35*, 972−983.
(6) Fujita, M.; Umemoto, K.; Yoshizawa, M.; Fujita, N.; Kusukawa, T.; Biradha, K. *Chem. Commun.* **2001**, *6*, 509−518.
(7) Cotton, F. A.; Lin, C.; Murillo, C. A. *Acc. Chem. Res.* **2001**, *34*, 759−771.
(8) Holliday, B. J.; Mirkin, C. A. *Angew. Chem., Int. Ed.* **2001**, *40*, 2022−2043.
(9) Swiegers, G. F.; Malefetse, T. J. *Chem. Rev.* **2000**, *100*, 3483−3538.
(10) Leininger, S.; Olenyuk, B.; Stang, P. J. *Chem. Rev.* **2000**, *100*, 853−908.
(11) Baxter, P. N.; Lehn, J. M.; Baum, G.; Fenske, D. *Chem. Eur. J.* **1999**, *5*, 102−112.
(12) Caulder, D. L.; Raymond, K. N. *J. Chem. Soc., Dalton Trans.* **1999**, 1185−1200.
(13) Caulder, D. L.; Raymond, K. N. *Acc. Chem. Res.* **1999**, *32*, 975−982.
(14) Fujita, M. *Chem. Soc. Rev.* **1998**, *27*, 417−425.
(15) Stang, P. J.; Olenyuk, B. *Acc. Chem. Res.* **1997**, *30*, 502−518.
(16) Lehn, J. M., Chair Ed. Board; Atwood, J. L., Davis, J. E. D., MacNicol, D. D., Vögtle, F. E. E., Eds. *Comprehensive Supramolecular Chemistry*; Pergamon Press: Oxford, U.K., 1996; Vols. 1−11.
(17) Stoddart, J. F., Ed. *Monographs in Supramolecular Chemistry 1−6*; Royal Society of Chemistry: Cambridge, U.K., 1989, 1991, 1994−1996.
(18) Desiraju, G. R. *Crystal Engineering: The Design of Organic Solids*; Elsevier: New York, 1989.
(19) Licheri, G.; Piccaluga, G.; Pinna, G. *Chem. Phys. Lett.* **1975**, *35*, 119−123.
(20) Licheri, G.; Piccaluga, G.; Pinna, G. *J. Chem. Phys.* **1976**, *64*, 2437−2441.

10.1021/ja0523690 CCC: $30.25

provides support for the existence of shape-persistent supramolecular macrocycles and three-dimensional cages. However, due to the rapid isotropic tumbling of the molecules in solution, NOE methods are confined to short (<6 Å) atom−atom distances. Therefore, further proof of the solution structure is highly desirable.

Traditionally, several spectroscopic (e.g., infrared and Raman) and diffraction methods (e.g., X-ray and neutron) have been employed to determine the coordination numbers and solvation shell of molecules and ions in solution. Coordination numbers, distances between atoms, and temperature factors of the atom pairs have been determined from the intensities of elastically scattered electrons, photons, and neutrons through atom bombardment. Inelastic scattering of electrons by atoms is small and therefore usually not considered in the diffraction measurements as a possible source of structural information. Wide-angle X-ray diffraction measurements have often been used for structure studies of liquids and solutions in systems called "simple liquids and solutions".[32,33] Aqueous or alcoholic solutions of small molecules (less than a few angstroms) have been examined by wide-angle X-ray diffraction.[34−36] Presently, X-ray and neutron diffraction methods are being utilized to examine ion pairing,[37−40] liquids and solutions under high pressure and temperature,[41−45] complexes which have complicated structures that are insoluble in water,[46,47] and even supramolecular assemblies.[48] However, with the development of computer programs to calculate solution X-ray scattering on the basis of atomic coordinates,[49−51] these techniques have recently been applied, as a complement to NMR spectroscopy, to probe the conformational state of proteins in solution.[51−58] Tiede and coworkers characterized the shape of a supramolecular host−guest porphyrin macrocycle using wide-angle scattering to 6 Å resolution.[48]

In this paper we demonstrate the use of wide-angle X-ray diffraction and NMR methods to establish the existence as well as the shape and size of our previously reported self-assembled metallacyclic rectangle (**2**),[59] triangle (**3**),[60] and D_{3h} molecular cage (**4**)[61] in solution (Figure 1).

Results and Discussion

Small-angle X-ray scattering was used to determine the overall sizes and shapes of the metallacyclic complexes, while large-angle scattering produces interference patterns. These interference patterns are then compared to the calculated scattering patterns to determine the conformation of these supramolecular complexes in solution. The solution structures are compared to the previously determined solid-state X-ray structures.

Low-Angle Region (0.12−2.48 Å^{-1}). Comparing the X-ray scattering curves of these complexes assisted with determining whether supramolecular complexes such as **2** are shape-persistent in solution. The low-angle X-ray scattering curves obtained, plotted as a function of the scattering variables k [$k = (4\pi/\lambda) \sin \Theta$], are shown in Figure 2. The atom−atom distances (r_n) can be calculated from k_n values of the maxima of scattered intensity on the basis of the equation $k_n r_n = \tan(k_n r_n)$.

The platinum−platinum distances calculated from the single-crystal X-ray data for the rectangle, triangle, and three-dimensional cage are reported in Table 1. The reported platinum−platinum distance for the half-rectangle was determined by modeling the molecule on the basis of the rectangle using the program Hyperchem version 6.0. For the rectangle **2**, a maximum of six platinum−platinum interactions are possible. However, only three interactions are expected to give rise to the peaks observed in the X-ray scattering curves recorded for this symmetrical complex, since the two short sides of the rectangle are equivalent (5.75 Å), as are the two long sides (11.3 Å) and the two diagonals (12.6 Å). Similarly, only six interactions are expected to be observed for **3** (7.7 Å × 3, 11.3 Å × 3, 15.4 Å × 2, 17.1 Å × 4, 18.04 Å × 2, and 20.82 Å × 1) and four for **4** (5.65 Å × 3, 10.65 Å × 5, 11.66 Å × 4, and 12.5 Å × 3), even though there are 15 total platinum−platinum interactions possible for each assembly.

(21) Caminiti, R.; Licheri, G.; Piccaluga, G.; Pinna, G. *J. Appl. Crystallogr.* **1979**, *12*, 34−38.
(22) Caminiti, R.; Licheri, G.; Piccaluga, G.; Pinna, G.; Radnai, T. *J. Chem. Phys.* **1979**, *71*, 2473−2476.
(23) Newsome, J. R.; Neilson, G. W.; Enderby, J. E.; Sandström, M. *Chem. Phys. Lett.* **1981**, *82*, 399−401.
(24) Cummings, S.; Enderby, J. E.; Howe, R. A. *J. Chem. Phys. C* **1980**, *13*, 1−8.
(25) Hewish, N. A.; Neilson, G. W.; Enderby, J. E. *Nature* **1982**, *297*, 138−139.
(26) Pálinkás, G.; Heinzinger, K. *Chem. Phys. Lett.* **1986**, *126*, 251−254.
(27) Yamaguchi, T.; Otaki, H.; Spohr, E.; Pálinkás, G.; Heinzinger, K.; Probst, M. M. *Z. Naturforsh. A* **1986**, *41A*, 1175−1185.
(28) Radnai, T.; Pálinkás, G.; Caminiti, R. *Z. Naturforsh. A* **1982**, *37A*, 1247−1252.
(29) Kalman, E.; Radnai, T.; Pálinkás, G.; Hajdu, F.; Vertes, A. *Electrochim. Acta* **1988**, *33*, 1223−1228.
(30) Probst, M. M.; Radnai, T.; Heinzinger, K.; Bopp, P.; Rode, B. M. *J. Phys. Chem.* **1985**, *89*, 753−759.
(31) Kameda, Y.; Ebata, H.; Usuki, T.; Uemura, O. *Physica B* **1995**, *213*, 477−479.
(32) Ohtaki, H.; Radnai, T. *Chem. Rev.* **1993**, *93*, 1157−1204.
(33) Marcus, Y. *Chem. Rev.* **1988**, *88*, 1475−1498.
(34) Ohtaki, H. *Pure Appl. Chem.* **1987**, *59*, 1143−1150.
(35) Johansson, G. *Adv. Inorg. Chem.* **1992**, *39*, 159−232.
(36) Yamaguchi, T. *Pure Appl. Chem.* **1990**, *62*, 2251−2258.
(37) Megyes, T.; Grósz, T.; Radnai, T.; Bakó, I.; Pálinkás, G. *J. Phys. Chem. A* **2004**, *108*, 7261−7271.
(38) Megyes, T.; Radnai, T.; Grósz, T.; Pálinkás, G. *J. Mol. Liq.* **2002**, *101*, 3−18.
(39) Jalilehvand, F.; Spångberg, D.; Lindqvist-Reis, P.; Hermansson, K.; Persson, I.; Sandström, M. *J. Am. Chem. Soc.* **2001**, *123*, 431−441.
(40) Gaspar, A. M.; Marques, M. A.; Cabaco, M. I.; de Barros Marques, M. I.; Buslaps, T.; Honkimaki, V. *J. Mol. Liq.* **2004**, *110*, 15−22.
(41) Radnai, T.; Megyes, T.; Bakó, I.; Kosztolányi, T.; Pálinkás, G.; Ohtaki, H. *J. Mol. Liq.* **2004**, *110*, 123−132.
(42) Ohtaki, H. *J. Mol. Liq.* **2003**, *103−104*, 3−13.
(43) Ohtaki, H.; Katayama, N.; Ozutsumi, K.; Radnai, T. *J. Mol. Liq.* **2000**, *88*, 109−120.
(44) Yamaguchi, K. *Pure Appl. Chem.* **1999**, *71*, 1741−1751.
(45) Ohtaki, H.; Radnai, T.; Yamaguchi, T. *Chem. Soc. Rev.* **1997**, *26*, 41−51.
(46) Megyes, T.; Schubert, G.; Kovács, M.; Radnai, T.; Grósz, T.; Bakó, I.; Pápai, I.; Horváth, A. *J. Phys. Chem. A* **2003**, *107*, 9903−9909.
(47) Megyes, T.; May, Z.; Schubert, G.; Simandi, L. I.; Radnai, T. *Inorg. Chim. Acta* **2005**, in press.
(48) Tiede, D. M.; Zhang, R.; Chen, L. X.; Yu, L.; Lindsey, J. S. *J. Am. Chem. Soc.* **2004**, *126*, 14054−14062.
(49) Svergun, D.; Barberato, C.; Koch, M. H. J. *J. Appl. Crystallogr.* **1995**, *28*, 768−773.
(50) Pavlov, M. Y.; Fedorov, B. A. *Biopolymers* **1983**, *22*, 1507−1522.
(51) Zhang, R.; Thiyagarajan, P.; Tiede, D. M. *J. Appl. Crystallogr.* **2000**, *33*, 565−568.
(52) Zuo, X.; Tiede, D. M. *J. Am. Chem. Soc.* **2005**, *127*, 16−17.
(53) Tiede, D. M.; Zhang, R.; Seifert, S. *Biochemistry* **2002**, *41*, 6605−6614.
(54) Botelho, M. G.; Gralle, M.; Oliveira, C. L. P.; Torriani, I.; Ferreira, S. T. *J. Biol. Chem.* **2003**, *278*, 34259−34267.
(55) Fischetti, R. F.; Rodi, D. J.; Mirza, A.; Irving, T. C.; Kondrashkina, E.; Makowski, L. *J. Synchrotron Radiat.* **2003**, *10*, 398−404.
(56) Gralle, M.; Botelho, M. G.; De Oliveira, C. L. P.; Torriani, I.; Ferreira, S. T. *Biophys. J.* **2002**, *83*, 3513−3524.
(57) Hirai, M.; Iwase, H.; Hayakawa, T.; Miura, K.; Inoue, K. *J. Synchrotron Radiat.* **2002**, *9*, 202−205.
(58) Svergun, D.; Petoukhov, M. V.; Koch, M. H. J. *Biophys. J.* **2001**, *80*, 2946−2953.
(59) Kuehl, C. J.; Songping, D. H.; Stang, P. J. *J. Am. Chem. Soc.* **2001**, *123*, 9634−9641.
(60) Kryschenko, Y. K.; Seidel, S. R.; Arif, A. M.; Stang, P. J. *J. Am. Chem. Soc.* **2003**, *125*, 5193−5198.
(61) Kuehl, C. J.; Kryschenko, Y. K.; Radhakirshnan, U.; Seidel, S. R.; Huang, S. D.; Stang, P. J. *Proc. Natl. Acad. Sci. U.S.A.* **2002**, *99*, 4932−4936.

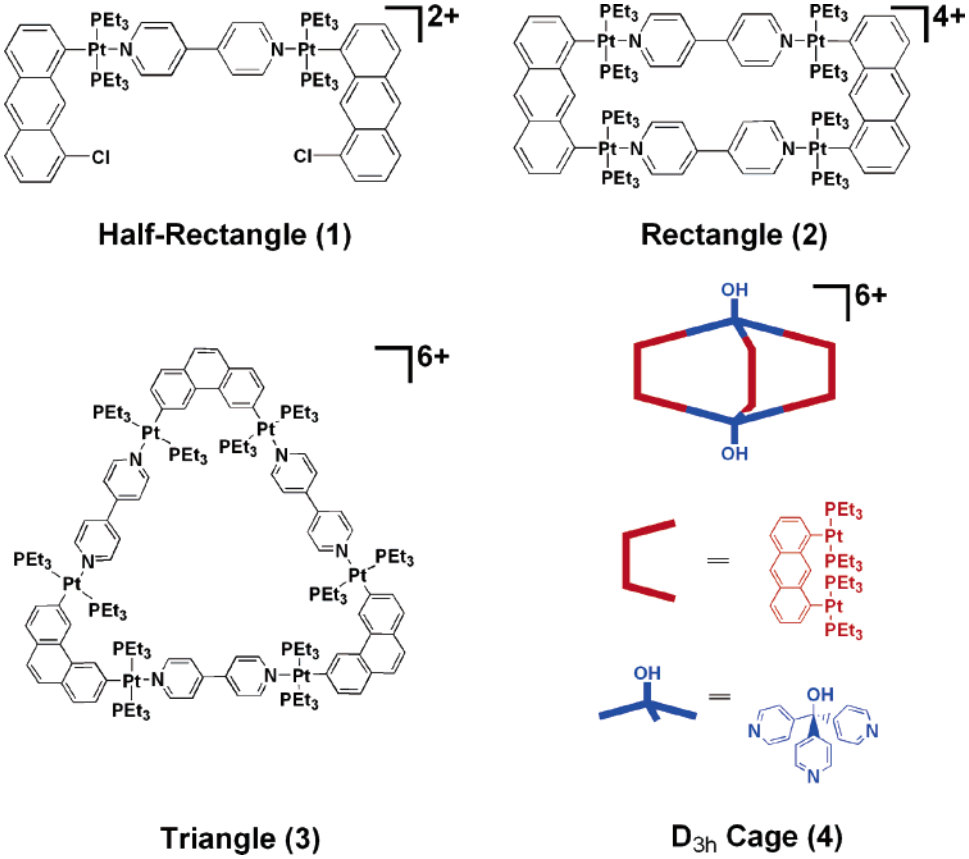

Figure 1. Molecular structures of supramolecular complexes **1**−**4**.

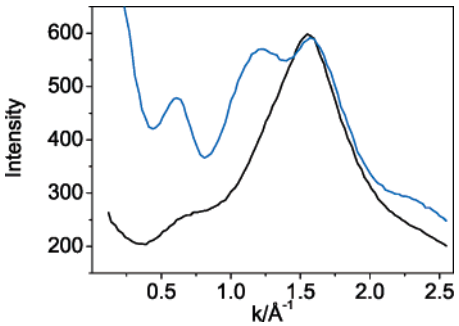

Figure 2. Corrected X-ray scattering patterns for **1** (black line) and **2** (blue line). Contributions from the long platinum−platinum distance give rise to the peak at 0.61 Å^{-1}. The second peak at 1.35 Å^{-1} (5.75 Å) is not observed in the scattering pattern of the half-rectangle because there is no short platinum−platinum interaction. The large peak at 1.7 Å^{-1} is due to solvent interactions.

Table 1. Platinum−Platinum Distances Calculated from the Previously Reported[59−61] Single-Crystal X-ray Data for the Supramolecular Complexes[a]

complex	platinum–platinum distances, Å	k_{cal}^{max}, Å^{-1}	k_{exp}^{max}, Å^{-1}
1	11.30	0.67	0.66
2	5.60, 11.30, 12.60	1.38, 0.67	1.40, 0.61
3	7.70, 11.30, 15.40, 17.10, 18.04	1.14, 0.82, 0.44	1.17, 0.81, 0.44
4	5.65, 10.65, 11.66, 12.09	1.14, 0.66	0.66

[a] Calculated (k_{cal}^{max}) and experimental (k_{exp}^{max}) scattering variables were determined from the scattering curves in Figure 3. The error in the distances is 0.01 Å.

The experimentally measured low-angle scattering curves for complexes **1**−**4** are compared with calculated scattering curves (1.4 Å^{-1} resolution) in Figure 3, and the data are listed in Table 1. The scattering curves were calculated using the program CRYSOL,[62] using single-crystal X-ray diffraction data[59−61] and accounting for solvent interactions. There is very good agreement between the experimental (k_{exp}^{max}) and calculated (k_{cal}^{max}) positions of the peaks which are due to the platinum−platinum interactions, suggesting that the assemblies are very similar in both the solution and solid states. Since it is not possible to include solvent−solvent and solvent−assembly interactions in the calculated curves, the peak intensities cannot be compared.

As expected for the half-rectangle, only one peak is observed, 0.67 Å^{-1}, corresponding to a platinum−platinum distance of 11.4 Å (Figure 3a). However, X-ray scattering curves measured on nitromethane solutions of the rectangle are not as simple as those observed for the half-rectangle (Figure 3b). First, the peak at 0.66 Å^{-1} is shifted to 0.61 Å^{-1}. This peak originates from four long platinum−platinum interactions in the rectangle, corresponding to the two sides (∼11.3 Å) and two diagonals (∼12.6 Å) of the rectangle. In addition to the peak at ∼0.61 Å^{-1}, a second peak is observed at 1.35 Å^{-1}, corresponding to two platinum−platinum interactions of 5.75 Å (short side of the rectangle) (Figure 3b). The scattering pattern for **2** has been deconvoluted, and the contributions of the solvent as well as intramolecular platinum−platinum interactions to the scattering curves of **2** are shown in Figure 4.

Three peaks are observed in both the measured and calculated X-ray scattering curves of **3** (Figure 3c). There is good agreement between the experimental and calculated scattering variables. The peak at 0.44 Å^{-1} corresponds to the six platinum−platinum interactions between 17.5 and 18 Å, the

(62) See Supporting Information for details about how the program was used.

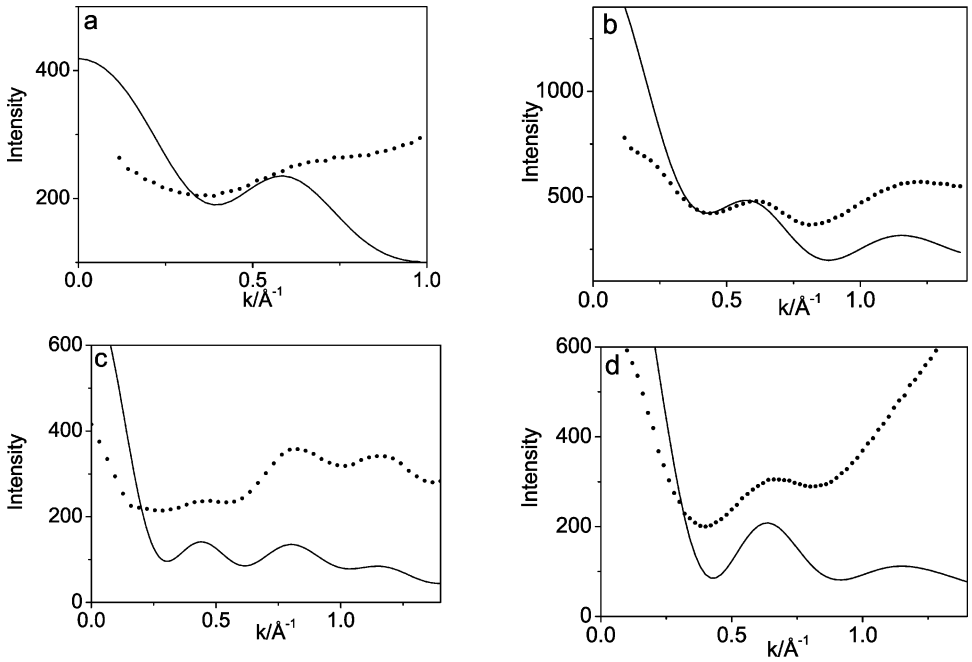

Figure 3. Calculated (solid line) and experimental (dotted line) X-ray scattering curves for nitromethane solutions of (a) **1**, (b) **2**, (c) **3**, and (d) **4**.

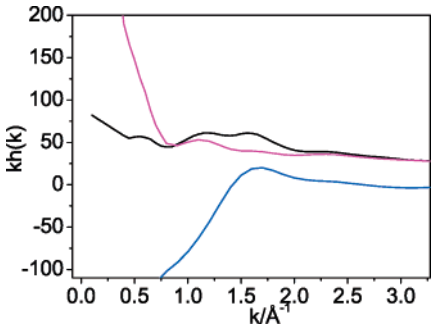

Figure 4. Deconvoluted structure function (black line) of **2**, and contributions from the solvent (blue line) and intramolecular platinum interactions in the complex (red line) to the scattering curves.

peak at 0.82 $Å^{-1}$ is due to the five platinum−platinum interactions between 11.3 and 15.5 Å, and the one at 1.14 $Å^{-1}$ is due to the three interactions of ∼7.70 Å. For the molecular cage **4** the agreement between the measured and theoretical X-ray scattering curves is less satisfactory (Figure 3d). The first peak (0.66 $Å^{-1}$), corresponding to a distance of 5.56 Å, is observed in both the calculated and experimental scattering curves. However, due to the poor solubility of the D_{3h} cage, the concentration of the solution studied is very low and the second peak, calculated at 1.14 $Å^{-1}$, is masked by the solvent peak and cannot be resolved.

Large-Angle Region (0.19−16 $Å^{-1}$). The low-angle region was successfully used to show that the supramolecular assemblies are shape-persistent in solution. However, due to the instrumental setup, it was not possible to collect data below 0.12 $Å^{-1}$, and therefore the radius of gyration could not be calculated. More direct structural information has been derived from the large-angle region. The measured structure functions $kh(k)$ are compared to the calculated intramolecular contributions from the supramolecular complex and the solvent in Figure 5. The theoretical contributions were calculated on the basis of the equations given in the Supporting Information. The contribution of the long-range interactions from the solvent ("continuum part") to the total scattering curve, based on neat liquid nitromethane, was calculated using eq S7. The total solvent contribution to the structure function of the solution was subtracted, and the resultant difference curves were compared to the intramolecular platinum−platinum contributions of the complexes. The platinum−platinum interactions occur between 0 and 7 $Å^{-1}$ in the measured and theoretical calculated structure functions (Figure 6). The similarity of the calculated and measured scattering curves is remarkable, considering that interactions between the molecular assembly and solvent were not taken into account. Due to the complexity of this system, further analysis of the interactions between the molecular assembly and solvent was not possible.

The pair correlation functions, $g(r)$, for **1**−**4** are shown in Figure 7. A visual inspection of the radial distribution functions indicates that they are composite and no peaks can be uniquely assigned to a specific interaction. The first two peaks in the pair correlation function are centered at ∼1.20 and ∼2.25 Å (Figure 7) for all four complexes. The solvent and anion interactions are short range (<3 Å) and most likely overlap to form these peaks.

The pair correlation functions in $r^2[g(r) - 1]$ representation are shown in Figures 8 and 9. The experimental platinum−platinum pair correlation functions (Figure 9) have been calculated and fitted to modeled pair correlation functions containing a sum of Gauss functions.[63] Platinum−platinum distances (r), mean square deviations (σ), and coordination number (n) were obtained for **2** and **3** and are given in Table 2.

As expected, no short platinum−platinum interactions are observed in the pair correlation function for the half-rectangle. However, the long platinum−platinum distance appears at 11.40(0.01) Å. The inset in Figure 8a contains the composition

(63) Details about the treatment of the experimental pair correlation function and the model pair correlation function are given in the Supporting Information.

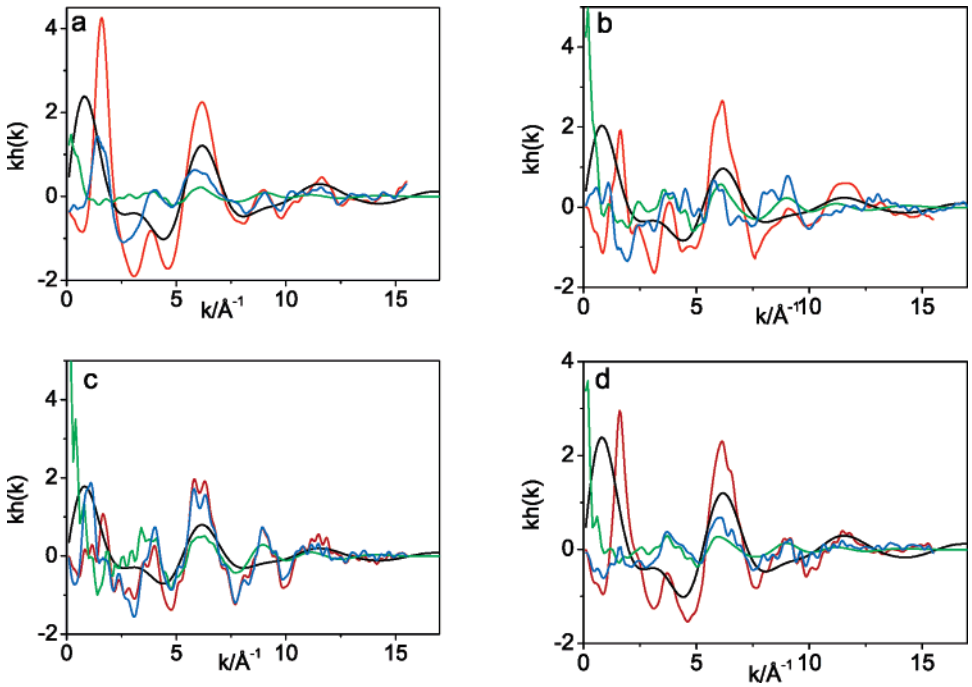

Figure 5. Structure functions $h(k)$ multiplied by k for (a) **1**, (b) **2**, (c) **3**, and (d) **4** supramolecular complexes in nitromethane solution. The difference curve (blue line) was obtained by subtracting the total solvent contribution from the measured structure function (red line). This difference curve is in agreement with the theoretical intramolecular contributions of the supramolecular complex (green line). The intramolecular solvent contributions are also shown (black line).

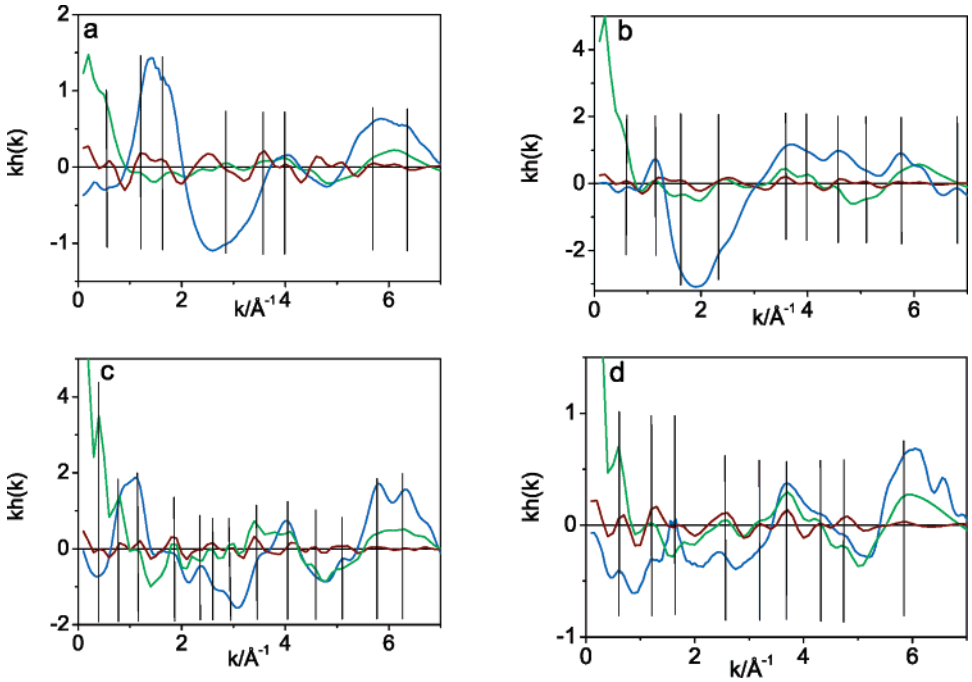

Figure 6. Structure functions $h(k)$ multiplied by k for (a) **1**, (b) **2**, (c) **3**, and (d) **4** in nitromethane solution. The difference structure function (blue line) is compared to the calculated intramolecular contributions of the supramolecular complex (green line) and to the platinum−platinum interaction (red line). For ease of comparison, the main peaks are marked with vertical lines.

of the peak between 9.5 and 13 Å. The platinum−platinum interaction is represented with a red line; the remaining three interactions occur between the molecular assembly and solvent.

The pair correlation function for the rectangle is shown in Figure 8b. Peaks at 5.60(0.01) and 11.30(0.01) Å correspond to the platinum−platinum distances along the short and long sides of the rectangle, respectively. The number of overlapping platinum−platinum interactions that give rise to these peaks, hereafter referred to as coordination number (n), was determined to be 2.10(0.01) and 2.29(0.20) for the peaks at 5.6 and 11.3 Å, respectively. The excellent agreement between the experimental and theoretical peaks suggests that the rectangle retains its shape in solution. However, the peaks corresponding to the diagonal platinum distance, determined to be 12.67(0.01) and 12.55(0.01) Å from the theoretical model, overlap and are observed at 12.47(0.03) Å [n = 1.98(0.03), Figure 9b]. The Pt−

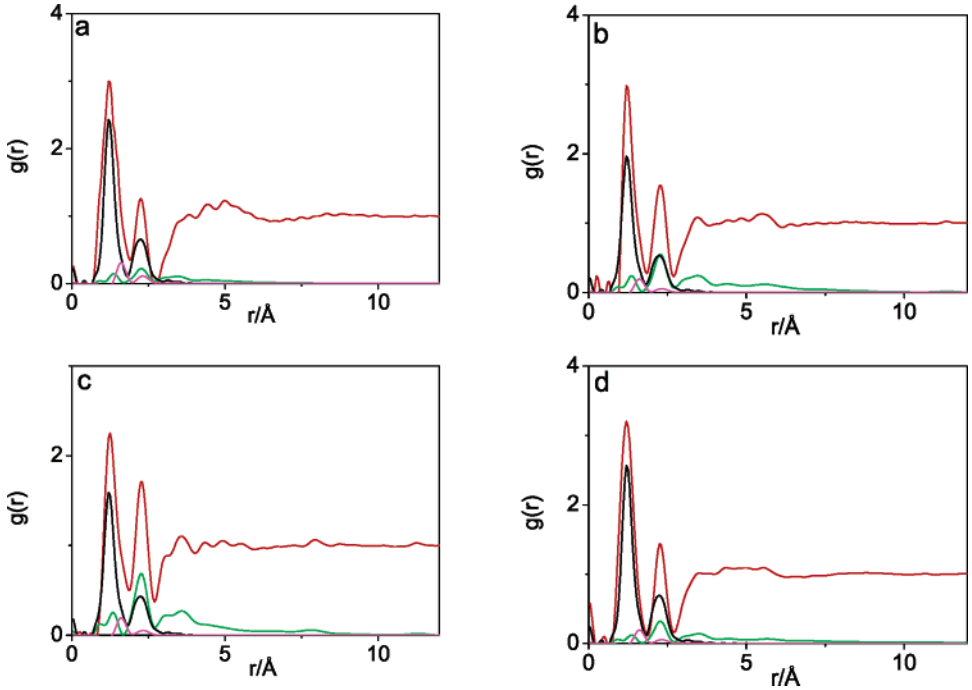

Figure 7. Pair correlation functions $g(r)$ for (a) **1**, (b) **2**, (c) **3**, and (d) **4** in nitromethane solution, showing the experimental (red line) and calculated supramolecular complex (green line), solvent (black line), and anion (pink line) intramolecular interactions in solution.

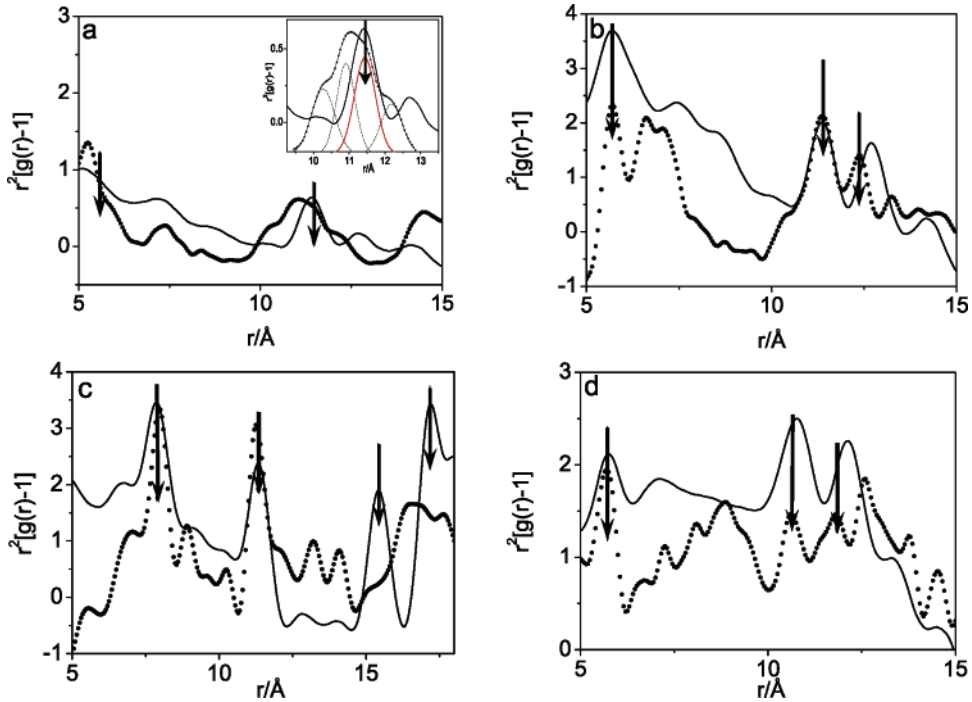

Figure 8. Experimental (dotted line) and calculated (solid line) pair correlation functions $r^2[g(r) - 1]$ for (a) **1**, (b) **2**, (c) **3**, and (d) **4** in nitromethane solution. The platinum−platinum contributions are indicated by arrows. The experimental pair correlation function for the half-rectangle was determined to arise from four overlapping peaks (panel a, inset, 9.5−13 Å): one corresponds to the platinum−platinum interaction (red), and the other three are due to complex−solvent interactions.

Pt−Pt angles of the rectangle were determined to be 90.9(1.0)° and 89.4(1.0)° in the single crystal, but they were found to be 88.7(1.0)° in nitromethane solutions of the rectangle. Taken together, these data suggest that the rectangle, while shape-persistent, is not as rigid in solution as in the crystalline state. Most likely, the rectangle is rather flexible in solution, and these experiments detect only an average structure.

Likewise, the experimental [7.70(0.01) and 11.25(0.01) Å] and theoretical [7.70(0.01) and 11.30(0.01) Å] platinum−platinum distances along the sides of the triangle, determined from the pair correlation function (Figure 8c) of a nitromethane solution, are in excellent agreement. Theoretical modeling, based on the single-crystal data, predicts that the nine platinum−platinum diagonals will be observed as four peaks [15.40(0.01)

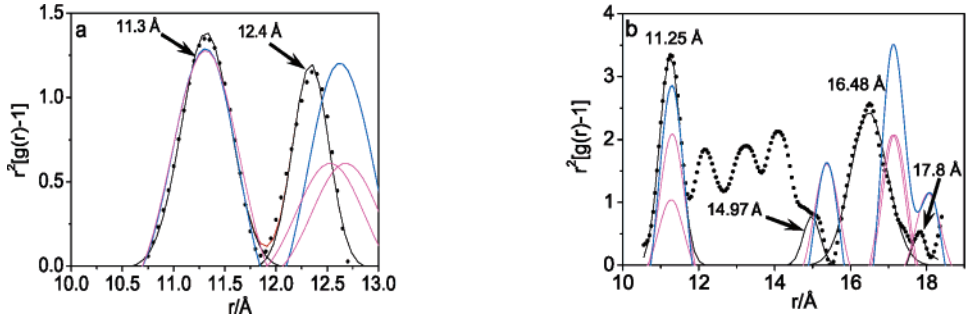

Figure 9. Total experimental (dotted line) and calculated (blue line) platinum−platinum pair correlation functions, $r^2[g(r) - 1]$, for (a) **2** and (b) **3** in nitromethane solution. Comparison with individual calculated (red line) and fitted (black line) platinum−platinum contributions confirms that the rectangle and triangle are virtually the same shape and size, both in solution and in the single crystal.

Table 2. Platinum−Platinum Distances (r), Mean Square Deviations (σ), and Coordination Number (n) for **2** and **3**

complex	r (Å)	σ (Å)	n
2	11.30(0.01)	0.49(0.01)	2.29(0.20)
	12.47(0.03)	0.42(0.03)	1.98(0.03)
	11.25(0.02)	0.52(0.01)	3.20(0.10)
3	14.97(0.03)	0.46(0.03)	2.20(0.10)
	16.48(0.05)	0.69(0.05)	5.92(0.10)
	17.80(0.05)	0.36(0.05)	1.08(0.10)

Å (two diagonals), 17.10(0.01) Å (four diagonals), 18.04(0.01) Å (two diagonals), and 20.82(0.01) Å (one diagonal)] in the pair correlation function. However, in the experimental data recorded for the nitromethane solutions of the triangle, the three peaks expected at 15.40(0.01), 17.20(0.01), and 18.01(0.01) Å overlap, and only a single peak at 16.50(0.01) Å is observed, with two shoulders at 14.97(0.01) and 17.80(0.01) Å. The individual interactions that contribute to the platinum−platinum interactions in the triangle are shown in Figure 9b. An average structure is observed with peaks corresponding to the platinum−platinum diagonal interactions at 14.97(0.01) Å, $n = 2.2$; 16.48-(0.02) Å, $n = 5.9$; and 17.80(0.01) Å, $n = 1.1$. As with **2**, these data suggest that **3**, while shape-persistent, is not as rigid in solution as in the crystalline state.

The partial correlation function for **4** is shown in Figure 8d. As observed for the previous three complexes, the platinum−platinum distances for the edges of the molecule, 5.70(0.01) and 10.60(0.01) Å, are the same in the single crystal and in solution. From the calculated scattering curve, a single peak corresponding to the diagonal platinum−platinum distances was expected to occur at 12.20(0.01) Å; however, peaks at 11.90(0.01) and 12.40(0.03) Å are observed in the scattering curve measured for a nitromethane solution of the D_{3h} cage. The peak positions corresponding to the interatomic platinum−platinum distances could be determined for this complex; however, due to its low solubility, the individual platinum−platinum contributions to the pair correlation function cannot be resolved, and the coordination number could not be determined.

Solution NMR Spectroscopy

The sizes of the molecular assemblies **1**−**4** were confirmed by DOSY NMR experiments.[64−66] The hydrodynamic radii calculated using the Einstein−Stokes equation[67] are given in Table 3. The large r values, which are in good agreement with the published molecular dimensions,[59−61] confirm that compounds **1**−**4** are intact supramolecular assemblies in solution. Compound **3** was determined to have the largest radius, while **2** and **4** were smaller and similar in size. We note that the radii in Table 3 are average molecular sizes which include the effect of the nearest solvation shells.

Table 3. Measured Diffusion Constants and the Calculated Hydrodynamic Radii for **1**−**4**[a]

compound	diffusion constant ($\times 10^{-10}$ m²/s, 293 K)	hydrodynamic radius (Å)
1	4.2 ± 0.1	8.3 ± 0.2
2	3.0 ± 0.1	11.5 ± 0.5
3	2.1 ± 0.2	16.5 ± 2.0
4	2.7 ± 0.1	12.8 ± 0.4
4,4′-bipyridyl	11.7 ± 0.2	3.0 ± 0.1
nitromethane-d_3	19.7 ± 0.7	1.8 ± 0.1

[a] Values for the ligand (4,4′-bipyridyl) and the solvent (nitromethane-d_3) are also given.

Conclusions

X-ray scattering measurements are proving to be a valuable technique for determining the shape and size of large molecules in solution. These measurements, used in conjunction with X-ray crystallographic and NMR methods, have been used to determine the solution structure of proteins.[55,57,58,68] Recently, Tiede and co-workers[48] were able to characterize the shape and size of a cyclic hexameric porphyrin host−guest assembly using X-ray scattering. Those authors determined that the porphyin host assembly underwent a 0.6 Å expansion upon guest insertion.

The work presented in this article demonstrates that wide-angle X-ray scattering can be used to obtain direct structural information about self-assembled supramolecular metallacyclic species in solution. Comparison of the measured and calculated low-angle scattering patterns confirms that **1**−**4** retain their shape when dissolved in nitromethane solution. Platinum−platinum distances and coordination numbers were obtained from the large-angle X-ray scattering patterns. Even though these supramolecular assemblies were found to be shape-persistent

(64) Morris, K. F.; Johnson, C. S., Jr. *J. Am. Chem. Soc.* **1992**, *114*, 3139−3141.
(65) Johnson, C. S., Jr. *Prog. Nucl. Magn. Reson.* **1999**, *34*, 203−256 and references therein.
(66) Wu, D.; Chen, A.; Johnson, C. S., Jr. *J. Magn. Reson. A* **1995**, *115*, 260−264.
(67) Delpuech, J.-J., Ed. *Dynamics of Solutions and Fluid Mixtures by NMR*; John Wiley and Sons Ltd.: New York, 1995.
(68) Petoukhov, M. V.; Eady, N. A.; Brown, K. A.; Svergun, D. I. *Biophys. J.* **2002**, *83*, 3113−3125.

in nitromethane solution, they are significantly less rigid in solution than in the single crystal. For example, the X-ray scattering peak for diagonal platinum−platinum interactions was found to be ∼0.15 Å smaller than expected on the basis of calculations from single-crystal X-ray data.

Acknowledgment. P.J.S. thanks the NIH (GM-57052) and the NSF (CHE-0306720) for financial support.

Supporting Information Available: Synthesis and analytical data for all new compounds; experimental method detailing programs and equations used to calculate theoretical scattering curves; figures showing raw and corrected X-ray scattering patterns for **1**−**4** and nitromethane; ^{1}H 2D-DOSY NMR spectra of **1**−**4** in nitromethane. This material is available free of charge via the Internet at http://pubs.acs.org.

JA0523690